

Fluidization of Spherical Particle Beds with Non-Newtonian Suspensions

I. Machač, B. Šiška, and L. Macháčová*

Department of Chemical Engineering,

*Institute of Mathematics, University of Pardubice,
nám. Čs. legií 565, 532 10 Pardubice, Czech Republic,
E-mail: Ivan.Machac@upce.cz

Original scientific paper
Received: February 9, 2005
Accepted: April 1, 2005

Fluidization of spherical particle beds with shear thinning fine particle suspensions has been investigated experimentally. The beds were composed of uniform glass, steel, and lead balls; the test liquids were suspensions of kaolin or titanium dioxide in water solutions of glycerol. The flow curves of suspension were approximated using power law and Herschel-Bulkley flow models. Overall, 61 particle-suspension-column systems were tested giving a Reynolds number range of $7 \times 10^{-4} \leq Re_{nt} \leq 43$.

Minimum fluidization velocities and the expansion of beds have been evaluated in creeping and transition flow regions. The equations based on power law and Herschel-Bulkley flow models have been suggested for the prediction of bed expansion course. It follows from the results obtained that the test suspensions can be treated as power law fluids and the use of Herschel-Bulkley flow model seems to be unnecessary for predicative calculations. Concerning the bed expansion relationships based on a capillary bed model, the best results are obtained if the dependence of tortuosity on the power law index is taken into account.

Keywords:

Solid-liquid fluidization, spherical particle beds, non-Newtonian suspensions, minimum fluidization velocity, bed expansion

Introduction

In our previous papers,¹⁻⁴ results have been presented for fluidization of spherical particle beds with different types of non-Newtonian fluids. It has been shown that the bed expansion may differ according to the kind of liquid media used.^{2,4,5} In the case of fluidization with viscoelastic polymer solutions, a reduction of the bed expansion has been observed due to the transition of the particulate fluidization to an aggregative one. Therefore, the expansion equations proposed in the literature^{e.g. 5, 6} for description of fluidization with purely viscous fluids must be applied to the fluidization with viscoelastic fluids with caution.

In this contribution, the results are summarized of our experimental investigations of fluidization of spherical particle beds with fine solid particle suspensions. The suspensions represent another important class of non-Newtonian fluids that can be encountered in the industrial applications of fluidized beds (e.g. bioreactors). The rheological behavior of suspensions is diverse and depends on many factors such as the nature of phases, solid particle concentration, particle size and shape, surface effects, and other possible interactions. The rheology of suspensions is briefly described, for example, in the literature.^{7,8} Concentrated suspensions of fine solid particles behave usually as shear-thinning fluids, they

often exhibit yield stress and their viscosity can also be time dependent. Thus, the aim of our investigations was to evaluate, whether, the relationships presented in the literature for the fluidization of spherical particle beds with purely viscous shear-thinning fluids may also be applied to fluidization with fine particle shear-thinning suspensions, and if the suspensions used as liquid media in our fluidization tests may be treated as power-law fluids.

Fundamentals

Expansion equations

The dependence of the voidage ε of a fluidized bed on the superficial liquid velocity u and on the liquid rheological behaviour is described by a bed expansion equation. Regarding the complexity of the fluid flow through a fluidized bed, the essential simplifications of the flow through the beds are used for developing expansion equations. To this purpose, the purely viscous rheological behaviour of non-Newtonian liquid and the particulate regime of fluidization (homogeneous fluidization) are usually supposed. At the same time, the attention is paid mostly to the description of expansion of spherical particle beds using capillary bundle or

submerged object approaches in combination with a suitable rheological model of the fluid.^{5,6}

For the sake of simplicity, the power law model

$$\frac{\tau}{\dot{\gamma}} = \eta(\dot{\gamma}) = K \cdot \dot{\gamma}^{n-1} \quad (1)$$

with parameters K and n is mostly used to express the viscosity function $\eta(\dot{\gamma})$ of a purely viscous fluid. Here, τ is the shear stress and $\dot{\gamma}$ is the shear rate. A variant of the power law for purely viscous fluids with yield stress τ_y is the Herschel-Bulkley model

$$\eta(\dot{\gamma}) = \frac{\tau_y}{\dot{\gamma}} + K \cdot \dot{\gamma}^{n-1}. \quad (2)$$

Capillary bed model

Various forms of the bed expansion equations based on a capillary bed model have been proposed in the literature for fluidization with a power law fluid.⁹⁻¹⁴

The bed resistance over a wide range of Reynolds number, including, both, creeping and inertial flow regions, is often considered to be the sum of the viscous and inertial resistance terms. Then, the resulting equation valid for expansion of spherical particle beds fluidized with a power law fluid may be written, for example, as

$$f = f_i(n, \varepsilon)_1 Re_n^{-1} + f_i(n, \varepsilon)_2, \quad (3)$$

where

$$f = \frac{g d (\rho_s - \rho) \varepsilon^3}{\rho u^2} \quad (4)$$

is the fluidized bed drag factor,

$$Re_n = \frac{d^n u^{2-n} \rho}{K} \quad (5)$$

is the power law Reynolds number, and $f_i(n, \varepsilon)_1$ and $f_i(n, \varepsilon)_2$ are the functions of the bed voidage ε and the flow index n . The forms of the functions $f_i(n, \varepsilon)_1$ and $f_i(n, \varepsilon)_2$, proposed by different authors, vary in dependence on the choice of the bed characteristic velocity u_{ch} and bed channel tortuosity t .

According to Mishra et al.⁹ and Kumar & Upadhyay,¹⁰ who have considered constant tortuosity $t = 25/12$ and characteristic velocity $u_{ch} = u/\varepsilon$, the functions $f_i(n, \varepsilon)_1$ and $f_i(n, \varepsilon)_2$ are given by relationships

$$f_M(n, \varepsilon)_1 = \frac{12.5 \left[\frac{(9n+3)(1-\varepsilon)}{n} \right]^n}{\varepsilon^{2(n-1)}} \quad (6)$$

and

$$f_M(n, \varepsilon)_2 = 1.75. \quad (7)$$

If the modified Reynolds number Re_{nb} is defined as

$$Re_{nb} = 150 [f_i(n, \varepsilon)_1]^{-1} Re_n, \quad (8)$$

eq. (3) may be (with $f_i(n, \varepsilon)_1 = f_M(n, \varepsilon)_1$ and $f_i(n, \varepsilon)_2 = f_M(n, \varepsilon)_2$) rewritten into the form

$$f = 150/Re_{nb} + 1.75 \quad (9)$$

analogous to the well-known Ergun equation for the flow through fixed beds.

Based on the results of measurements of expansion of spherical particle beds with water suspensions of titanium dioxide, Brea et al.¹¹ have proposed that for $Re_{nb} < 40$ (determined at the incipient of fluidization) the constant 150 in eq. (9) should be replaced by coefficient $121(1+5.65 d/D)$ or by the constant 140 ($t = 1.94$), if the wall effects are neglected.

Considering that the bed channel tortuosity depends on the bed voidage, $t = t(\varepsilon)$, and the inertial part of the bed drag factor is the same as that proposed for Newtonian fluids by Comiti & Reanaud,¹⁵ the functions $f_i(n, \varepsilon)_1$ and $f_i(n, \varepsilon)_2$ are according to Sabiri et al.¹² and Ciceron et al.¹³ expressed as

$$f_{SC}(n, \varepsilon)_1 = \frac{6[t(\varepsilon)]^{n+1} \left[\frac{(9n+3)(1-\varepsilon)}{n} \right]^n}{\varepsilon^{2(n-1)}} \quad (10)$$

and

$$f_{SC}(n, \varepsilon)_2 = 0.581[t(\varepsilon)]^3. \quad (11)$$

At the same time, they assume that the dependence of the tortuosity upon the bed voidage may be expressed as

$$t(\varepsilon) = 1 - p \ln \varepsilon, \quad (12)$$

where p is the parameter depending on the shape of particles in the bed. For beds of spherical particles $p = 0.49$.

For a viscoplastic fluid obeying the Herschel-Bulkley model (2), the form of expansion equation analogous to eq. (3) may be expressed as¹⁶

$$f = f_i(n, \varepsilon)_1 Re_{HB}^{-1} + f_i(n, \varepsilon)_2, \quad (13)$$

where

$$Re_{HB} = (1-X) \left[(1-X)^3 + \frac{2(3n+1)X(1-X)^2}{2n+1} + \frac{(3n+1)X^2(1-X)}{n+1} \right]^n Re_n \quad (14)$$

is the Reynolds number modified for a Herschel-Bulkley fluid,

$$X = \tau_y / \tau_w \quad (15)$$

$$\tau_w = r_h \frac{\Delta p}{L_{ch}} = \frac{d g (\rho_s - \rho) \varepsilon}{6 t} \quad (16)$$

is the mean shear stress at the channel wall, r_h is the hydraulic radius of the bed, Δp is the pressure drop across the bed, and L_{ch} is the characteristic length of bed channel.

Expansion equations based on the concept of flow around a submerged particle

Irrespective of the way used for estimation of the drag force, this class of expansion equations proposed for fluidization with a power law fluid is frequently presented in terms of dimensionless variables as

$$u/u_t = f_n(Re_{nt}, n, \varepsilon, d/D). \quad (17)$$

Here

$$Re_{nt} = \frac{d^n u_t^{2-n} \rho}{K} \quad (18)$$

is the power law Reynolds number based on the terminal falling velocity u_t . Special forms of eq. (18) for fluidization with purely viscous non-Newtonian fluids are presented, for example, in the works,^{5,6} experimental forms of the equations for fluidization with pseudoplastic and partly elastic polymer solutions are given in the works.²⁻⁵

For fluidization with a Herschel-Bulkley fluid, the expansion equation written in the form analogous to the relationship (17) can be expressed as

$$u/u_t = f_{HB}(Re_{HBt}, N_{HBt}, n, \varepsilon, d/D). \quad (19)$$

Here

$$Re_{HBt} = Re_{nt}(1 + N_{HBt})^{-1} = \frac{d^n u_t^{2-n} \rho}{K + \tau_y (d/u_t)^n} \quad (20)$$

is the particle Reynolds number modified for Herschel-Bulkley fluid and

$$N_{HBt} = \frac{\tau_y}{K} \left(\frac{d}{u_t} \right)^n \quad (21)$$

is the plasticity number modified for Herschel-Bulkley fluid.

Minimum fluidization velocity

The minimum fluidization velocity u_{mf} can be predicted from the equations of expansion substitut-

ing the minimum fluidization bed voidage ε_{mf} for ε or from the special equations proposed to that purpose.⁵ For example, the following simple relationships were proposed by Machač et al.^{2,5} for fluidization with shear-thinning fluids

$$\text{for } Re_{nt} \leq 0.3 \quad u_{mf}/u_t = 0.018 \quad (22)$$

and

$$\text{for } 0.3 < Re_{nt} < 165 \quad u_{mf}/u_t = 0.024 Re_{nt}^{0.2}. \quad (23)$$

Experimental

The aim of the experiments performed in our laboratory^{16,17} was to investigate the expansion of spherical particle beds fluidized with non-Newtonian fine particle suspensions and to evaluate the relationships for the description of bed expansion, and for prediction of minimum fluidization velocity for this type of fluidization.

In the experiments, the expansion of beds was observed in two Perspex cylindrical columns of 2 and 4 cm in diameter at the temperature nearly 20 °C (± 0.5 °C). During experiments, the height of the bed and the pressure drop were measured in dependence on the volume flow rate of suspension. The beds were composed of uniform glass, steel, and lead balls; their diameters and densities are given in Tab. 1. The height of the beds at the onset of fluidization was about 15 cm. The distributor (sieve plate with holes of 1 mm in diameter) with free area of 20 % was used. The test liquids were suspensions of kaolin KKN or titanium dioxide RD-54 in water solutions of glycerol. The solid mass fraction ranged from $w = 6$ to 17 % in suspensions of kaolin; in suspensions of titanium dioxide the solid mass fraction was $w = 30$ % (see Tab. 2).

Table 1 – Characteristics of spherical particles used

Symbol	Material	Diameter d/mm	Density $\rho/\text{kg m}^{-3}$
S 1	glass	1.92	2524
S 2	glass	2.78	2504
S 3	glass	4.12	2596
S 4	steel	3.17	7854
S 5	steel	3.97	7826
S 6	steel	4.73	7927
S 7	lead	1.97	11090
S 8	lead	2.85	11190

Table 2 – Characteristics of test suspensions, 20 °C

Symbol	Suspension composition w/%	Density $\rho/\text{kg m}^{-3}$	Power law		Shear rate range $\dot{\gamma} / \text{s}^{-1}$	Herschel-Bulkley model		
			K Pa s^n	n –		τ_y Pa	K Pa s^n	n –
UL 1	68 % glycerol, 17 % H ₂ O, 15 % kaolin	1289	6.99	0.356	1.5-40.5	8.03	1.93	0.613
			6.50	0.383	5.4-81.0	7.82	1.32	0.710
UL 2	68.5 % glycerol, 17 % H ₂ O, 14.5% kaolin	1284	5.15	0.406	9.0-72.9	6.21	1.05	0.722
UL 3	72 % glycerol, 18 % H ₂ O, 10 % kaolin	1267	1.75	0.464	1.5-16.2	1.88	0.630	0.732
			1.39	0.553	16.2-48.6	1.77	0.657	0.727
UL 4	74 % glycerol, 18 % H ₂ O, 8 % kaolin	1259	0.712	0.663	27.0-72.9	0.513	0.473	0.753
			0.618	0.698	40.5-146	0.546	0.481	0.756
UL 5	75 % glycerol, 19 % H ₂ O, 6 % kaolin	1253	0.347	0.755	1.5-16.2	0.208	0.249	0.837
			0.312	0.786	27.0-146	0.201	0.241	0.840
UL 6	54 % glycerol, 16 % H ₂ O, 30 %TiO ₂	1491	0.0917	0.829	9.0-48.6	0.182	0.0762	0.844
			0.107	0.782	121.5-364	0.101	0.0969	0.802
UL 7	35 % glycerol, 35 % H ₂ O, 30 %TiO ₂	1437	1.17	0.245	2.7-16.2	1.28	0.159	0.689
			0.320	0.575	146-656	1.22	0.167	0.664
ML1	88 % glycerol, 4 % H ₂ O, 8 % kaolin	1289	0.863	0.960	8.1-365	0	0.863	0.960
ML2	83 % glycerol, 3 % H ₂ O, 14 % kaolin	1338	2.80	0.810	3.0-48.6	0.642	2.42	0.852
ML3	77 % glycerol, 8.5 % H ₂ O, 14.5 % kaolin	1313	2.73	0.640	3.0-81.0	0.301	2.55	0.652
ML4	80 % glycerol, 3.4 % H ₂ O, 16.6% kaolin	1339	7.43	0.520	1.5-27.0	4.07	4.31	0.663

The suspensions were prepared by gradual dispersion of powdered kaolin or titanium dioxide into water solutions of glycerol. The dispersion of solid was achieved using the mixer Etamira (6000 rpm) in the experiments of *Ulbrichová*¹⁶ and using the turbine impeller (2000 rpm) in the experiments of *Matura*.¹⁷ The rheological characteristics of the suspensions were measured on the rotary cylindrical viscometer Rheotest 2, which allowed measurements in the range of shear rate $1.5 \leq \dot{\gamma} \leq 1312 \text{ s}^{-1}$, after each bed expansion experiment. The content, density, and examples of the power law and Herschel-Bulkley model parameters of the test suspensions are given in Tab. 2. Terminal velocities of particles falling through opaque test suspensions were measured using two different methods.^{16, 18} The terminal velocities of all test particles (irrespective of their material) were determined (once for all) making use of a video-radiography method. The measurement of terminal falling velocities of steel balls was repeated after each bed expansion

experiment detecting the particle position by two electromagnetic coils mounted on the column. Overall, 61 particle-suspension-column systems were tested giving a Reynolds number range of $7 \times 10^{-4} \leq Re_{nt} \leq 43$.

Results and Discussion

Rheological characteristic of test suspensions

The examples of shear stress-shear rate dependences (flow curves) are shown for individual test suspensions in Fig. 1. The flow curves were fitted to the power law (eq. (1)) and Herschel-Bulkley (eq. (2)) flow models. Since the power law model fits the suspension viscometric data with sufficient accuracy over a limited interval of shear rates only, the parameters n and K were evaluated from the viscometric data in the range of shear rates corresponding to those reached in the fluidization experi-

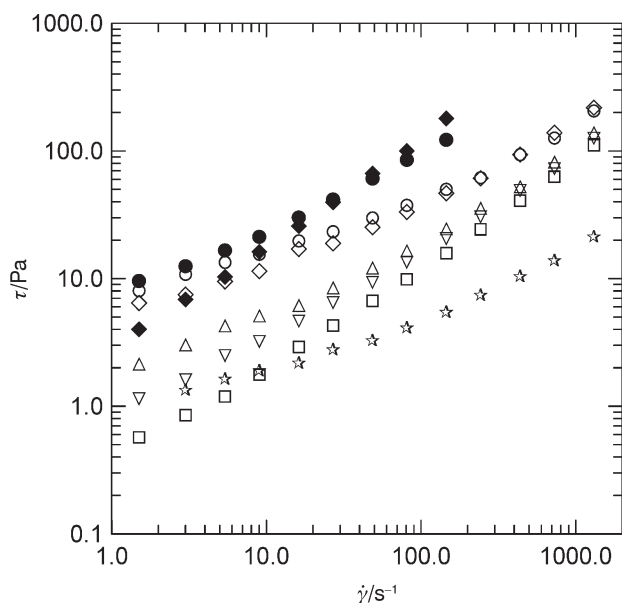


Fig. 1 – Examples of shear stress-shear rate dependencies for test suspensions: (*) ML4; (◆) ML3; (○) UL1; (◇) UL2; (Δ) UL3; (∇) UL4; (□) UL5; (☆) UL7

ments. This range was estimated according to the relation

$$\dot{\gamma} \cong \frac{12u(1-\varepsilon)}{d\varepsilon^2} \frac{3n+1}{4n} \quad (24)$$

substituting the corresponding maximum and minimum experimental values of superficial velocity and bed voidage for velocity u and voidage ε . The parameters of Herschel-Bulkley model were determined making use of all viscometric data available. The examples of parameters obtained are given for both aforementioned models in Tab. 2. It should be noted that the values of τ_y given in Tab. 2 are treated as fitted parameters and do not represent the true yield stress of suspensions tested. The more fraction suspensions (over $w = 10\%$) of kaolin showed also a slight degree of thixotropy.

The influence of fluidization temperature on fluidized bed expansion is above all determined by dependence of liquid rheological properties on temperature. We note that the effect of temperature on viscosity of suspensions is not unambiguous. The suspension viscosity can fall, remain unchanged, or rise with increase in temperature.⁸ In this work, the influence of temperature on viscosity function of model suspensions has not been investigated.

Bed expansion

For evaluation of expansion course of individual systems measured, the experimental results have been plotted in the form of dependencies $\log(u/u_t) = f(\log \varepsilon)$ (expansion curves). In this manner,

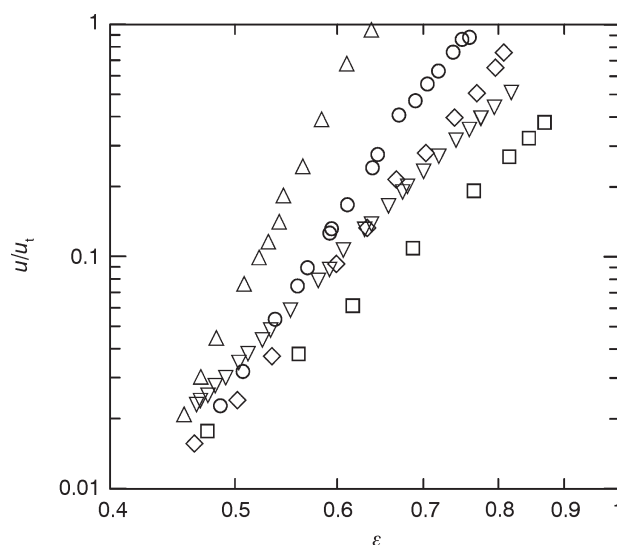


Fig. 2 – Examples of expansion curves measured in the creeping flow region: (Δ) UL7-S1, $n = 0.245$, $d/D = 0.05$; (○) UL2-S4, 0.430, 0.08; (∇) UL5-S2, 0.803, 0.07; (◇) ML2-S4, 0.810, 0.08; (□) ML0-S1, 1.00, 0.05

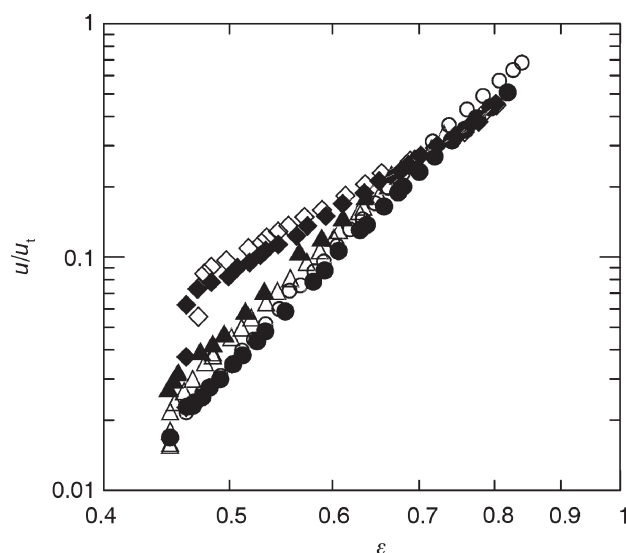


Fig. 3 – Examples of expansion curves for transition flow region: (○) UL3-S7, $Re_{nt} = 0.56$, $n = 0.587$; (λ) UL5-S2, 0.41, 0.803; (Δ) UL5-S4, 5.4, 0.790; (▲) UL4-S5, 5.4, 0.700; (◇) UL6-S5, 43, 0.767; (◆) UL6-S4, 41, 0.795

the expansion course of beds fluidized with liquids differing by their rheological behaviour can be clearly compared. Examples of the expansion curves obtained are shown in Figs. 2 and 3.

It has been found, that the expansion curves can be in a log-log plot approximated by straight lines for all systems tested. However, unlike the fluidization with Newtonian fluids, rather different expansion course has been observed in the creeping flow region ($Re_{nt} < 0.3$).

It can be seen from Fig. 2 that the slopes (index) z of the expansion straight lines increases

along with the decreasing power law index n . This fact corresponds with a reducing bed expansion, which gives evidence of rising occurrence of non-uniformities in the beds with the increasing suspension pseudoplasticity.

The observed expansion course is apparently caused by influence of the anomalous liquid rheological behaviour accompanied with eventual wall and distributor effects. The results of our previous investigation of the influence of distributor construction on the quality of non-Newtonian fluidization³ indicate, that the distributor used in this work will not affect significantly the expansion course. However, considering that in our experiments values of the ratio d/D ranged from 0.048 to 0.237, the evident wall effects may be expected. The wall effects can manifest themselves, both, by the shifting of expansion curves and by dependence of index z on the ratio d/D .^{19,20} At the same time, the shifting of expansion curves is dominant and the dependence of index z on d/D can be, for Newtonian solid-liquid fluidization in the range $0 < d/D < 0.25$, neglected.^{3,19}

The values of index z , determined for individual systems measured from bed expansion experimental data, are for the creeping flow region shown in dependence on the quantity $(1-n)$ in Fig. 4. It follows from this figure that, beside the flow index n , the values of z in a certain measure depend on the ratio d/D . Considering that the dependence

$$z = k_1 + k_2(1-n)(1-d/D)^{k_3} \quad (25)$$

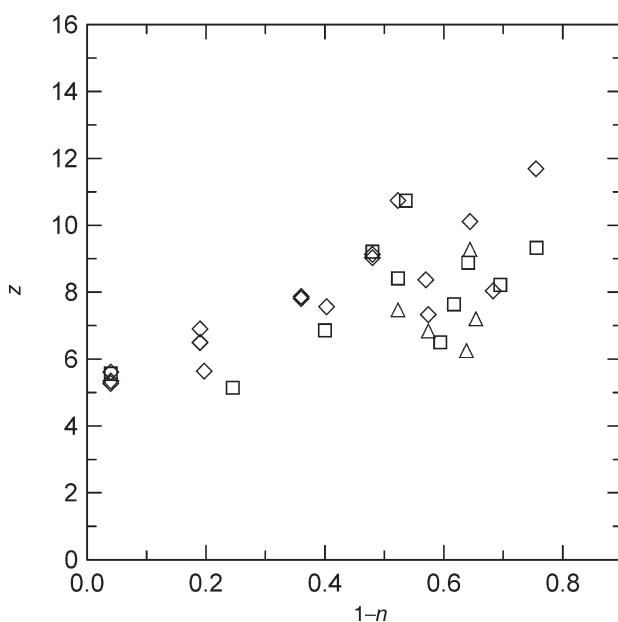


Fig. 4 – Dependence of the exponent z on the quantity $(1-n)$ for fluidization in the creeping flow region: (◇) 0.04 d/D 0.09; (Δ) 0.09 d/D 0.15; (□) 0.16 d/D 0.24.

correlates the experimental data of z , it was found by optimisation of parameters $k_1 - k_3$, that the values of these parameters can be taken as

$$k_1 = k_2/2 = k_3 = 5.0. \quad (26)$$

Then, the mean relative deviation of the experimental values of z and those calculated using the eq. (25) with parameters $k_1 - k_3$ expressed by eq. (26) is 8.3 %. We note that the excess of index z attributed to the liquid non-Newtonian behaviour decreases with increasing value of d/D (see Fig. 4).

Unlike the creeping flow region, it was found that the values of z , evaluated from experiments carried out in the transition flow region ($0.3 \leq Re_{nt} \leq 43$), do not depend significantly on the suspension power law index n . These experimental values can be correlated by the equation

$$z = \left(5.4 - 1.25 \frac{d}{D}\right) Re_{nt}^{-0.1}. \quad (27)$$

At the same time, the dependence of the exponent z on the Reynolds number is analogous to that found for Newtonian fluidization.⁶

The above discussed bed expansion experimental data indicate that the simple power law model (1) can be successfully used for characterisation of rheological behaviour of the test suspensions during fluidization. Regarding the linearity of expansion curves in a log-log plot and considering that the expansion straight lines start from the point of incipient of fluidization, the simplest empirical form of the expansion equation can be written as

$$\frac{u}{u_{mf}} = \left(\frac{\varepsilon}{\varepsilon_{mf}}\right)^z. \quad (28)$$

For predicative bed expansion calculations using eq. (28), the knowledge of the values of minimum fluidization velocity u_{mf} and minimum fluidization bed voidage ε_{mf} (see next section) is, of course, needed. The eq. (28) can be rewritten in the terms of terminal falling velocity as

$$\frac{u}{u_t} = k \varepsilon^z, \quad (29)$$

where

$$k = \frac{u_{mf}}{u_t} \varepsilon_{mf}^{-z}. \quad (30)$$

Then, eq. (29) represents a modified form of the well-known Richardson-Zaki expansion equation.^{3,4,19}

In order, to evaluate also the usability of eq. (3) for the prediction of expansion of spherical particle

beds fluidized with fine particle suspensions, the individual experimental values of the bed voidage ε (about 1000 data points) were compared with those calculated according to eq. (3), using functions $f_i(n, \varepsilon)_1$ and $f_i(n, \varepsilon)_2$, proposed by *Mishra et al.*⁸ and *Sabiri et al.*¹¹ The agreement between experimental and predicted data of the bed voidage has been evaluated according to the mean relative deviations

$$\delta_m = \frac{1}{N} \sum_{j=1}^N |\delta_j| \quad (31)$$

where

$$\delta_j = \frac{\varepsilon_c - \varepsilon_e}{\varepsilon_e} \cdot 100 \% \quad (32)$$

are the individual relative deviations of the experimental and calculated values of bed voidage. The obtained values of the total deviations δ_m are summarised in Tab. 3. It followed from the results of comparison of deviations δ_m obtained for individual systems tested, that the values of bed voidage ε predicted according to eq. (3) with functions $f_i(n, \varepsilon)_1$ and $f_i(n, \varepsilon)_2$ given by relationships (6) and (7) can be in the creeping flow region loaded with significant errors, especially for low values of suspension flow index n and high values of ε . In this case, the values of ε are overestimated. However, satisfactory results yield the aforementioned relationships for the prediction of ε in the transition flow region. At the same time, eqs. (10), (11), and (12), proposed by *Sabiri et al.*¹¹ and *Ciceron et al.*,¹² yield the better results in the creeping flow region to compare with those in the transition flow region. Due to limited validation of the eqs. (10), (11), and (12) for fluidization with purely viscous fluids^{11, 12, 21}, the values of ε calculated using eqs. (10), (11), and (12) are for higher values of the ratio u/u_t underestimated in the transition region. These facts are documented in Figs. 5 and 6 where the experimental courses of expansion curves are compared with the predicted ones for the systems UL2-S8 (creep-

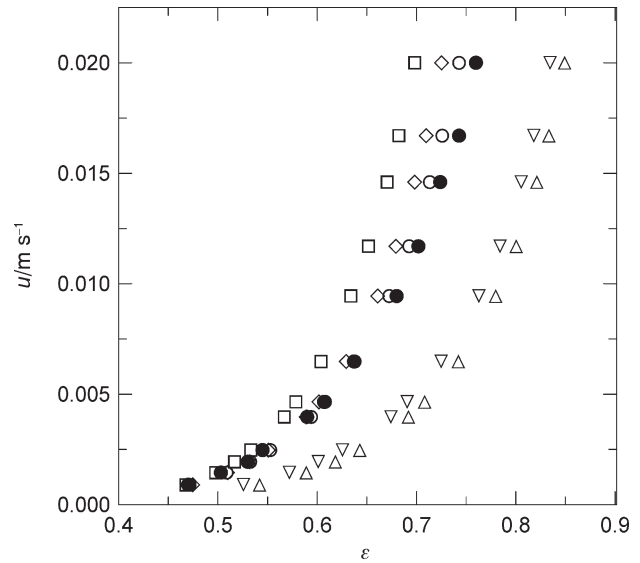


Fig. 5 – Comparison of the experimental course of expansion curve with the predicted ones for the system UL2-S8: $Re_{nt} = 0.042$; (λ) experiments; (Δ) eq. (3) along with functions $f_i(n, \varepsilon)_1$ and $f_i(n, \varepsilon)_2$ according to *Mishra et al.*,⁹ and *Kumar and Upadhyay*,¹⁰ (∇) eq. (3) along with functions $f_i(n, \varepsilon)_1$ and $f_i(n, \varepsilon)_2$ according to *Brea et al.*,¹¹ (\diamond) eq. (3) along with functions $f_i(n, \varepsilon)_1$ and $f_i(n, \varepsilon)_2$ according to *Sabiri et al.*¹² and *Ciceron et al.*,¹³ (\circ) eq. (3) along with eqs. (10), (11), (33), and (34) (this work); (\square) eq. (28) along with eqs. (25) and (26) (this work).

ing flow region) and UL7-S7 (transition flow region).

It can be expected that a better accordance between experimental and calculated bed expansion data will be reached if the geometrical tortuosity t , occurring in eqs. (10) and (11), is treated as a hydraulic tortuosity,²¹ and its dependence upon the flow index n (eventually on the ratio d/D as well) is assumed. Regarding difficulties with a theoretical expression of this dependence, the best way of its evaluation is experiment. Calculating the values of tortuosity t from bed expansion experimental data, it has been found that these experimental values can be (in the measured interval of ε) simply approximated by the relationship

$$t = 1 + p/\varepsilon \quad (33)$$

Table 3 – Mean relative deviations δ_m between experimental and calculated data of bed voidage

	$\delta_m/\%$			
	eqs. (6) and (7) (<i>Mishra et al.</i> ⁹)	eq. (3)	eqs. (10), (11), and (12) (<i>Sabiri et al.</i> ¹²)	eqs. (10), (11), (33), and (34) (this work)
creeping flow region	12.0	5.5	5.3	4.4
transition flow region	4.8	6.2	3.1	2.7
total	7.5	5.9	3.9	3.3

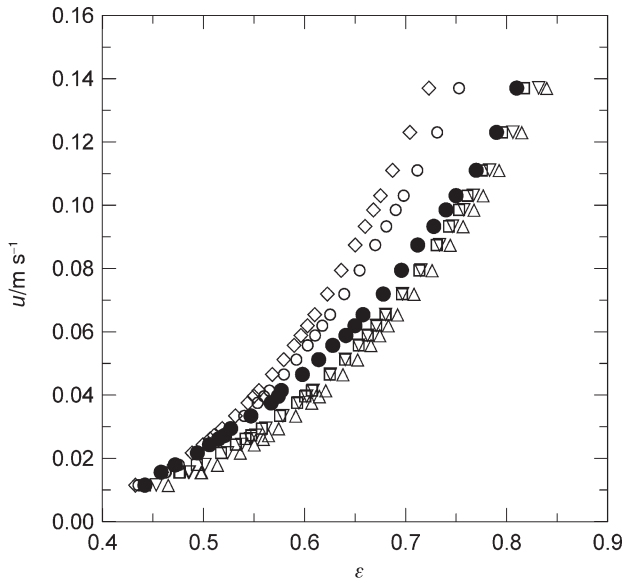


Fig. 6 – Comparison of the experimental course of expansion curve with the predicted ones for the system UL7-S7: $Re_{nt} = 17.7$; (●) experiments; (Δ) eq. (3) along with functions $f_i(n, \varepsilon)_1$ and $f_i(n, \varepsilon)_2$ according to Mishra et al.⁹, and Kumar and Upadhyay¹⁰; (▽) eq. (3) along with functions $f_i(n, \varepsilon)_1$ and $f_i(n, \varepsilon)_2$ according to Brea et al.¹¹; (◇) eq. (3) along with functions $f_i(n, \varepsilon)_1$ and $f_i(n, \varepsilon)_2$ according to Sabiri et al.¹² and Ciceron et al.¹³ (○) eq. (3) along with eqs. (10), (11), (33), and (34) (this work); (□) eq. (28) along with eq. (27) (this work).

with

$$p = 0.549 - 0.183(1-n)^{0.33} - 0.264 \left(1 - \frac{d}{D}\right)^2. \quad (34)$$

The relative deviations of the experimental values of bed voidage and those calculated making use of eq. (3), (10), (11), (33), and (34) are given in Tab. 3. It follows from Tab. 3 that if the eq. (3) is used for the bed voidage calculation, the most accurate prediction of expansion course gives the exploitation of eqs. (10) and (11) along with eqs. (33) and (34).

The results of expansion experiments can also be fitted with very good accuracy (especially in the transition flow region) by eq. (13), based on the Herschel-Bulkley flow model (2), along with eqs. (10), (11), and (33), if the coefficient p in eq. (33) is given as

$$p = 0.549 - 0.168 N_{HB}^{0.1} - 0.183 \left(1 - \frac{d}{D}\right)^2, \quad (35)$$

where

$$N_{HB} = \frac{\tau_y d^n}{K u_{mf}^n} \quad (36)$$

is the plasticity number calculated at the onset of fluidization.

Regarding the aforementioned favourable results of employing the power law model, however, the use of the more complicated eq. (13) for predictive calculations of expansion of spherical particle beds fluidized with the examined types of suspensions seems to be unnecessary.

Minimum fluidization velocity

The experimental values u_{mf} of minimum fluidization velocities and the corresponding values ε_{mf} of bed voidage at the onset of fluidization were evaluated from the course of experimental expansion curves.¹ The obtained values of ε_{mf} were ranged in the interval from 0.433 to 0.492. They can be with the mean relative deviations 2.1 %, approximated by linear dependence

$$\varepsilon_{mf} = 0.446 + 0.103 d/D. \quad (37)$$

The experimental data of u_{mf} have been compared with those predicted making use of eq. (3), substituting ε_{mf} for bed voidage ε , and also making use of the following relationships proposed by Machač et al.² for fluidization with polymer solutions

$$\text{for } Re_{nt} \leq 0.3 \quad u_{mf}/u_t = 0.018 \quad (38)$$

and

$$\text{for } 0.3 < Re_{nt} < 165 \quad u_{mf}/u_t = 0.024 Re_{nt}^{0.2}. \quad (39)$$

The discrepancy between experimental and calculated minimum fluidization velocity data is shown in Fig. 7. For creeping flow region, the mean deviations between experimental u_{mf} data and those calculated according to eq. (3) are ranged in the interval from 29 % to 70 %. The minimum value has been obtained for $f_i(n, \varepsilon)_1$ and $f_i(n, \varepsilon)_2$ expressed by eqs. (10), (11), and (33) with constant value $p = 0.29$, the maximum one for $f_i(n, \varepsilon)_1$ and $f_i(n, \varepsilon)_2$ given by eqs. (10), (11), and (12) with $p = 0.49$. In the transition flow region, eq. (3) yields much better results of u_{mf} prediction in comparison with those obtained in the creeping flow region. In this case, the mean deviations between experimental and calculated u_{mf} data, ranged in the interval from 10 % ($f_i(n, \varepsilon)_1$ and $f_i(n, \varepsilon)_2$ are given by eqs. (6) and (7)) to 26 % ($f_i(n, \varepsilon)_1$ and $f_i(n, \varepsilon)_2$ are given by eqs. (10), (11), and (12) with $p = 0.49$). The use of eq. (38) or (39) gives the mean deviations between experimental and calculated u_{mf} data of 15 % for the, both, creeping and transition flow regions.

Substituting the experimental values of u_{mf} and ε_{mf} into eq. (28) and using eqs. (25) or (27) for expression of the exponent z , the accuracy of the eq. (28) has also been evaluated for calculation of fluidized bed voidage. In this case, the total mean

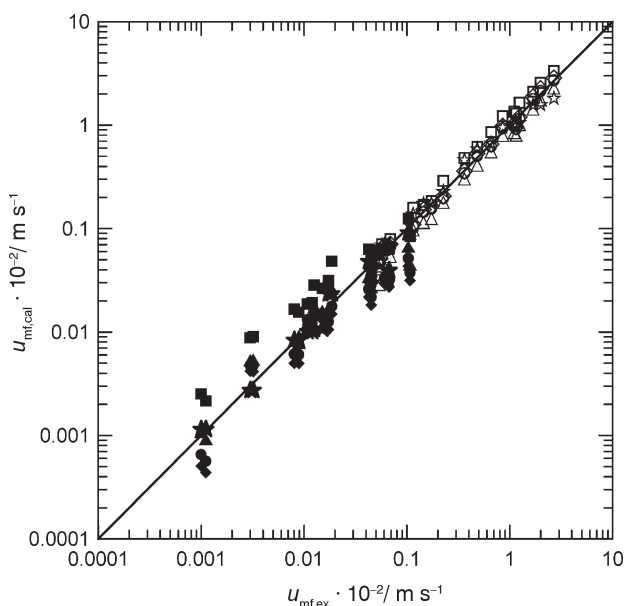


Fig. 7 – Comparison of the experimental minimum fluidization velocity data with the calculated ones: (○) eq. (3) along with functions $f_i(n, \varepsilon_{mf})_1$ and $f_i(n, \varepsilon_{mf})_2$ according to Mishra et al.,⁹ and Kumar and Upadhyay;¹⁰ (◇) eq. (3) along with functions $f_i(n, \varepsilon_{mf})_1$ and $f_i(n, \varepsilon_{mf})_2$ according to Brea et al.¹¹; (□) eq. (3) along with functions $f_i(n, \varepsilon_{mf})_1$ and $f_i(n, \varepsilon_{mf})_2$ according to Sabiri et al.¹² and Ciceron et al.;¹³ (Δ) – eq. (3) along with eqs. (10), (11), (33), and constant value $p = 0.29$ (this work); (☆) – eqs. (37) or (38); solid symbols – creeping flow region; open symbols – transition flow region.

relative deviations of experimental and calculated values of ε were 2.3 % for the creeping flow region and 3.6 % for the transition flow region. Substituting coefficient k given by eq. (30), calculated using eqs. (25), (37), and (38) (creeping flow region) or (27), (37), and (39) (transition flow region), into eq. (29), the resulting values of mean relative deviations between experimental and calculated bed voidage data were 3.7 % for the creeping flow region and 3.9 % for the transition flow region.

Conclusions

The transition from a fixed bed into a fluidized bed state and the expansion of spherical particle beds fluidized with shear thinning fine particle suspensions were investigated in creeping and transition flow regions. In the both regions, log-log plots of experimental expansion curves can be approximated by straight lines. The slope z of these expansion straight lines depends on the degree of suspension non-Newtonian anomaly and on the wall effects in the creeping flow region. In the transition flow region, the dependence of z on the Reynolds number is, like for fluidization with Newtonian liquids, dominant.

Equations based on power law and Herschel-Bulkley flow models were suggested for the prediction of the bed expansion course. Regarding the satisfactory results of exploitation of power law model for fine particle suspensions tested, the use of the more complicated relationships based on the Herschel-Bulkley flow model seems to be unnecessary for predicative calculations. Concerning bed expansion relationships, based on a capillary bed model, the best results are obtained (especially in the creeping flow region) if the dependence of tortuosity t on the power law index n is taken into account. At the same time, relatively good predictions in the transition flow region yield equations of Mishra et al.⁹

The proposed expansion equations may also be used for prediction of the minimum fluidization velocity u_{mf} substituting the value ε_{mf} for bed voidage ε . It was found that the special simple eqs. (38) and (39), suggested for prediction of minimum fluidization velocity for fluidization with shear thinning and elastic polymer solutions, give also acceptable results for fluidization with suspensions.

It was found that shear-thinning fine particle suspensions may be treated in fluidization as power-law fluids. The equations proposed in this work for prediction of minimum fluidization velocity and spherical particle bed expansion can be exploited as a basis for design calculations of two-phase (eventually three-phase) fluidized bed reactors with fine particle suspensions as continuous phase. Fluidized bed design aspects, incorporating distributor effects, are given, for example, in the book.²²

ACKNOWLEDGEMENT

We acknowledge partial financial support received from the Grant Agency of the Czech Republic (Grant Project No. 104/03/0544).

Notation

- d – particle diameter, m
- D – column diameter, m
- f – bed drag factor defined by eq. (4)
- $f_i(n, \varepsilon)_1$ – function of the bed voidage ε and the flow index n
- $f_i(n, \varepsilon)_2$ – function representing the inertial part of the bed drag factor
- g – gravity acceleration, m s^{-2}
- k – coefficient
- $k_1 - k_3$ – coefficients
- K – power-law parameter, Herschel-Bulkley model parameter, Pa s^n
- L_{ch} – characteristic length of the bed, m

- n – power-law parameter, Herschel- Bulkley model parameter
- N_{HB} – plasticity number
- N_{HBt} – plasticity number for a particle fall, eq. (21)
- p – coefficient
- Δp – pressure drop, Pa
- r_h – hydraulic radius of the bed, m
- Re_n – power-law Reynolds number, eq. (5)
- Re_{nt} – power-law Reynolds number for a particle fall
- Re_{nb} – power-law Reynolds number
- Re_{HB} – Reynolds number modified for Herschel-Bulkley fluid
- t – tortuosity
- u – superficial velocity, $m\ s^{-1}$
- u_t – particle terminal falling velocity, $m\ s^{-1}$
- u_{ch} – characteristic liquid velocity, $m\ s^{-1}$
- u_{mf} – minimum fluidization velocity, $m\ s^{-1}$
- w – mass fraction, %
- X – ratio of the Herschel-Bulkley model parameter τ_y and the shear stress τ_w
- z – slope of the expansion straight lines in log-log coordinates
- $\dot{\gamma}$ – shear rate, s^{-1}
- δ_i – individual relative deviation
- δ_m – mean relative deviation
- ε – bed voidage
- ε_{mf} – bed voidage at the incipient of fluidization η viscosity, Pa s
- ρ – density, $kg\ m^{-3}$
- ρ_s – particle density, $kg\ m^{-3}$
- τ – shear stress, Pa
- τ_w – mean shear stress at the channel wall, Pa
- τ_y – Herschel-Bulkley model parameter, Pa

Subscripts

- c – calculated
- e – experimental
- i – related to the authors
- M – related to the authors
- SC – related to the authors

References

1. Machač, I., Balcar, M., Lecjaks, Z., *Chem. Eng. Sci.* **41** (1986) 591.
2. Machač, I., Mikulášek, P., Ulbrichová, I., *Chem. Eng. Sci.* **48** (1993) 2109.
3. Machač, I., Šiška, B., Lecjaks, Z., Bena, J., *Chem. Eng. Sci.* **52** (1997) 3409.
4. Machač, I., Comiti, J., Brokl, P., Šiška, B., *Trans IChemE* **81**, Part A (2003) 1217.
5. Chabra R. P., Comiti, J., Machač, I., *Chem. Eng. Sci.* **56** (2001) 1.
6. Chhabra, R. P., *Bubbles, drops, and particles in non-Newtonian fluids*, CRC Press, Boca Raton, 1993, pp 299-330.
7. Barnes, H. A., Hutton, J. F., Walters, K., *An Introduction to Rheology*, Elsevier, Amsterdam, 1989, pp. 115-139.
8. Ferguson, J., Kemblowski, Z., *Applied fluid rheology*, pp. 199-231, Elsevier, London, 1991.
9. Mishra, P., Singh, D., Mishra, J. M., *Chem. Eng. Sci.* **30** (1975) 397.
10. Kumar, S., Upadhyay, S. N., *Ind. Eng. Chem. Fundam.* **20** (1981) 186.
11. Brea, F. M., Edwards, M. F., (Wilkinson, W. L., *Chem. Eng. Sci.* **31** (1976) 329.
12. Sabiri, N. E., Comiti, J., Brahimi, M., *Proceedings of the Fifth World Congress of Chemical Engineering*, San Diego, California, 1996.
13. Cicéron, D., Sabiri, N. E., Comiti, J., *13th International Congress CHISA'98*, Prague, 1998.
14. Dolejš, V., Mikulášek, P., *Chem. Eng. Proc.* **36** (1997) 111.
15. Comiti, J., Renaud, M., *Chem. Eng. Sci.* **44** (1989) 1539.
16. Ulbrichová, I., Ph.D. Thesis, Institute of Chemical Technology of Pardubice, Pardubice, 1994 (in Czech).
17. Matura, M., Diploma Work, Institute of Chemical Technology of Pardubice, Pardubice, 1986 (in Czech).
18. Machač, I., Ulbrichová, I., Elson, T. P., Cheesman, D. J., *Chem. Eng. Sci.* **50** (1995) 3323.
19. Khan, A. R., Richardson, J. F., *Chem. Eng. Sci.* **45** (1990) 255.
20. Neužil, L., Hrdina, M., *Collection Czechoslov. Chem. Commun.* **30** (1965) 752.
21. Cicéron, D., Comiti, J., Chabra R. P., Renaud, M., *Chem. Eng. Sci.* **57** (2002) 3225.
22. Gupta, C. K., Sathiyamoorthy, D., *Fluid Bed Technology in Material Processing*, CRC Press, Boca Raton, 1999.